e-J. Surf. Sci. Nanotech. Vol. 9 (2011) 6-14 Conference - NC-AFM2010 -

Polarized Tips or Surfaces: Consequences in Kelvin Probe Force Microscopy*

T. Hynninen† and A. S. Foster
Department of Physics, Tampere University of Technology, P.O. Box 692, FI-33101 Tampere, Finland and Department of Applied Physics, Aalto University School of Science, P.O. Box 11100, FI-00076 Aalto, Finland

C. Barth‡
Centre Interdisciplinaire de Nanoscience de Marseille, CNRS, Campus de Luminy, Case 913, 13288, Marseille Cedex 09, France

(Received 30 September 2010; Accepted 5 January 2011; Published 15 January 2011)

In this work, we present non-contact atomic force microscopy (nc-AFM) and Kelvin probe force microscopy (KPFM) simulations of the (001) surface of silver and supported MgO thin films. From the calculated force spectroscopy, we predict atomic resolution at tip-surface distances of less than 5 Å. For KPFM, we study the influence of charges localized on either the tip or on the surface on the Kelvin voltage. It is shown that the Kelvin voltage changes when the tip is placed above an MgO monolayer, only if the layer has a permanent net dipole. For point charges on the silver surface we examine the lateral resolution in the distance range of 1 to 3 nm, which is the standard working distance in KPFM. We show that point charges appear as nanometer large spots in Kelvin images, which is due to a long-range electrostatic interaction with the tip apex. [DOI: 10.1380/ejssnt.2011.6]

Keywords: Atomic force microscopy; Kelvin probe force microscopy; Charge detection; Density functional calculations; Magnesium oxides; Thin insulating films

I. INTRODUCTION

Kelvin probe force microscopy (KPFM) [1–3] has become a standard technique in atomic force microscopy (AFM) for many scientific disciplines [4, 5]. If the AFM is used in the noncontact mode (nc-AFM) [6] and in ultra-high vacuum (UHV) [7, 8] KPFM allows measurement of the variations in the local surface work function with a high lateral resolution in the meV range. The surfaces of metals, semiconductors [9] or of thin insulating films supported on metal surfaces [10–12] can be measured regardless of the presence of supported metal nanoclusters [13] or molecules [14]. The lateral resolution depends on the dimension of the tip-apex and the objects supported on the surface [12, 15, 16], and in some cases an atomic scale contrast can be observed [17]. Not only work function changes, but also the charge distribution on insulator surfaces [18, 19] and their influence on nano-objects like metal nanoclusters [20, 21] can be precisely measured with this technique. The sensitivity of the Kelvin microscope is sufficiently high that even surface charges below the equivalent charge of one electron can be detected [19, 22, 23].

In a recent work, we presented experiments and simulations which deal with nc-AFM and KPFM of thin MgO(001) films on Ag(001) [12]. Such thin MgO films play an important role as magnetic tunnel junctions or as dielectrics in electronic devices [24, 25], and as a support material for metal clusters in catalysis [26–29]. A particular difficulty of this surface system during nc-AFM imaging is the ever present possibility of tip changes due to exchange of MgO material between the tip and the surface. A strong consequence is that the tip can change its charge state by picking up ions or dipoles from the surface. Only stoichiometric, neutral tips image the correct topography of the surface, whereas charged or polar tips considerably change the topography contrast. The charge state of the tip, which is characterized by the sign and strength of the charge or dipole at the tip, can be effectively measured with help of the mean Kelvin voltage [30]. Therefore, in addition to being able to estimate the geometry of the tip [16], KPFM is an excellent tool to distinguish charged/polar tips from neutral ones. Since the tip can pick up ions or dipoles on any ionic surface during nc-AFM imaging, the experimental procedure proposed in Ref. 30 is quite useful for any experiment on ionic surfaces. Once the charge state of the tip is determined by KPFM, a Kelvin-identified-tip (KIT) helps in the interpretation of the imaging contrast in nc-AFM.

In this work, we expand our model for a further description of neutral, charged and polar tips in nc-AFM and KPFM. We present numerical simulations of the chemical short-range and electrostatic KPFM interaction between different types of tips with the silver surface and supported MgO monolayers. First, we show that the chemical interaction dominates the tip-surface interaction for distances below 5 Å but can be neglected for larger distances. In the second part we further examine our electrostatic model from Ref. 30 and show that when charges are included into the tip-surface system, long range electrostatic interactions result from the coupling of charges, in either the tip or on the surface, to the capacitive potential created by the external bias voltage. A discussion about the influence of a polar MgO film on the Kelvin

*This paper was presented at the 13th International Conference on Non-Contact Atomic Force Microscopy (NC-AFM2010), Ishikawa Ongakudo, Kanazawa, Japan, 31 July-4 August, 2010.
†Corresponding author: teemu.hynninen@tut.fi
‡Corresponding author: barth@cinam.univ-mrs.fr

voltage and the image contrast of fixed charges on the silver surface is involved. The latter is important from the perspective of charged defects in thin MgO films like F+ and F++ centers and charged adatoms, which locally change the electrostatic surface potential [31, 32].

II. METHODS

A. Force spectroscopy

Force spectroscopy calculations were performed using spin-polarized density functional theory (DFT) and the generalized gradient approximation (GGA) as implemented in the plane-wave code VASP [33]. Projected augmented wave potentials were used. The potentials for the elements were generated in the configurations $[1s^2]2s^22p^4$ for O, $[He2s^2]2p^63s^2$ for Mg, and $[Kr]4d^{10}5s^1$ for Ag, with the core electrons given in brackets. Energy cutoff of 400 eV was used, and k-points were generated in a $2 \times 2 \times 1$ Monkhorst-Pack grid [34], which resulted in energy convergence to a precision of approximately 10 meV. The Ag and MgO/Ag surfaces were modeled as slabs of four and five atomic layers, respectively, with their (001) surfaces exposed. For both cases, the two lowermost layers were frozen to mimic bulk Ag. Atomic force microscope tips were modeled as tetrahedral Ag_{20} and cubic $Mg_{32}O_{32}$ clusters, to mimic stoichiometric Ag, O, and Mg terminated nanotips. Also non-stoichiometric MgO tips were simulated using $Mg_{31}O_{29}$ and $Mg_{29}O_{31}$ clusters (truncated cubes). Although the part of the tip closest to the surface was the same for both stoichiometric and non-stoichiometric tips, the dipole moments of the non-stoichiometric tips were much larger (about 8 Debye) than those of the stoichiometric counterparts (1 Debye). These simulations contained no macroscopic part of the tip.

Forces acting on the tips were determined for tip-surface distances of around 2 to 6 Å. The top parts of the clusters representing the tips were always kept frozen in order to fix the tip distance. The geometries of the rest of the tip and the surface were allowed to relax so that forces acting on the (non-frozen) ions converged to less than 0.02 eV/Å. The forces acting on the tips can be measured by calculating the force sum acting on either the whole tip (F_z^{all}) or just the frozen part (F_z^{frozen}). These should be the same within convergence accuracy, but they may differ due to accumulation of errors. Therefore, we calculate both and take the average $(F_z^{\mathrm{all}} + F_z^{\mathrm{frozen}})/2$. In figures, we give the difference $|F_z^{\mathrm{all}} - F_z^{\mathrm{frozen}}|/2$ as error bars to show an estimate of the numeric accuracy.

B. Kelvin probe force microscopy

Kelvin probe simulations were carried out using atomistic pair-potentials and the shell model of electrons with the SciFi code [35, 36]. Metallic electrodes were handled as continuum material. The silver substrate was modeled as an infinite metal plate and the macroscopic part of the AFM tip as a metallic sphere of a given radius R, usually 10 nm, as shown in Figure 1. Under the macrotip, different kinds of nanotips were included in atomistic detail

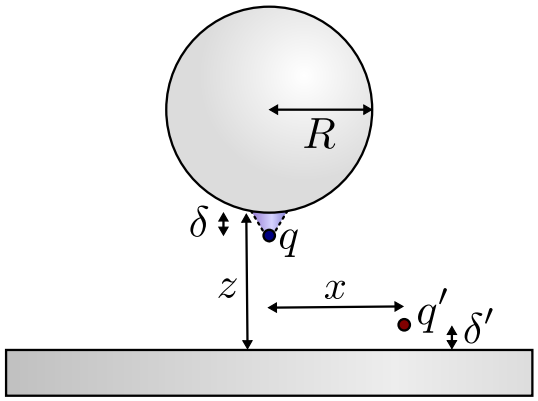

FIG. 1: The sphere-plate model. The macrotip is modeled as a conducting sphere of radius R, at a distance z from the metallic surface, treated as an infinite conducting plane. Below the sphere, an atomistic nanotip (distance δ, charge q) may be included. Likewise on the surface, charged species (q') can be introduced as ions.

as small clusters of Mg and O ions or neutral Ag atoms. Rectangular MgO films of one monolayer height were also included as islands of 24×24 ions, with the Mg and O species having the ideal charges of +2 and -2 e, respectively. The atomistic geometries were prerelaxed with the tip being far from the surface, but were then frozen as the tip distance range of 5 to 30 Å was probed.

We examine the effect of introducing localized charges in the KPFM system using the AFM image charge model by Kantorovich *et al.* [35]. As charges are brought into the system, they induce polarization in the capacitor formed by the spherical tip and the metallic surface. Thus a charge will interact with other charges and the resulting polarization, including the polarization induced by the charge itself. Denoting the electrostatic potential due to point charge q_j and the polarization it induces, felt by charge q_i (another point charge), as ϕ_{ij}, the energy of the collection of point charges can be written as $\sum_{i,j} q_i\phi_{ij}/2$. In SciFi, polarization of the electrodes is treated by an image charge expansion. The tip and the sample form a sphere-plate capacitor with an effective energy $-CU^2/2$, where $U = U_{\mathrm{dc}} + U_{\mathrm{CPD}}$ is the total voltage between the tip and the sample: a sum of the applied bias voltage U_{dc} and contact potential difference U_{CPD}. Here, also the energy of the batteries generating the bias are included. Naturally, also the point charges couple to the capacitor field. Denoting the potential of the capacitor felt by the point charge q_i by $\phi_i(U)$, the capacitor-point charge energy can be written as $\sum_i q_i\phi_i(U)$. Combining, the total energy of the system, the derivative of which yields the force acting on the tip, is

$$E = \frac{1}{2}\sum_{ij} q_i\phi_{ij} + \sum_i q_i\phi_i(U) - \frac{1}{2}CU^2 \quad (1)$$

$$= u_0 + u_1U + u_2U^2. \quad (2)$$

The latter equation is merely a shorthand, where the coefficients are $u_0 = \sum_{i,j} q_i\phi_{ij}/2$, $u_1 = \sum_i q_i\phi_i(U)/U$, and $u_2 = -C/2$. Assuming a static geometry, the coefficients u_i depend on the tip distance, but not on the voltage ($\phi(U) \propto U$, so u_1 is a constant as well). Then, the energy has the typical parabolic dependence on the bias.

KPFM may be operated in modes which are sensitive to either the force $F_z = -\partial E/\partial z$ (AM-mode) or the force gradient $F_z' = -\partial^2 E/\partial z^2$ (FM-mode) [37, 38]. According to (2), both quantities are parabolic with respect to U, with the coefficients u_i replaced by the corresponding derivatives $-\partial u_i/\partial z$ or $-\partial^2 u_i/\partial z^2$. In both cases, the KPFM apparatus effectively tries to find the bias U^{Kelvin} that yields the extremum of the corresponding quantity. For parabolic curves, these extrema are given simply by [30]

$$U_{\text{AM}}^{\text{Kelvin}} = -\frac{1}{2}\frac{\partial u_1}{\partial z}\Big/\frac{\partial u_2}{\partial z} \quad (3)$$

$$U_{\text{FM}}^{\text{Kelvin}} = -\frac{1}{2}\frac{\partial^2 u_1}{\partial z^2}\Big/\frac{\partial^2 u_2}{\partial z^2}. \quad (4)$$

The coefficients u_i can be extracted numerically by calculating the force acting on the tip (or the total energy) for a range of biases U and tip distances z. The Kelvin voltages are then obtained through a numeric differentiation of the coefficients and equations (3) and (4). Here we ignore effects coming from cantilever dynamics although they may influence the averaged electrostatic forces in KPFM [39].

In addition to the numeric approach, analytic expressions may be derived for the coefficients u_i. The capacitance of a sphere-plate capacitor is well described by the expression $C = 2\pi\varepsilon R(2+\ln(1+R/z))$ [40], which gives u_2. It is not straightforward to estimate u_1 for an arbitrary charge distribution, but for the special case of a point charge q on the nanotip, at a distance δ below the spherical macrotip, the expression $u_1 = q\phi(U)/U|_{z-\delta} = q\delta/z$ is obtained assuming a linearly changing potential between the tip and the surface with the tip grounded [30]. Using equations (3) and (4) the Kelvin voltage for a charged tip may thus be written as

$$U_{\text{AM}}^{\text{Kelvin}} = \frac{q\delta}{2\pi\varepsilon R^2}(1 + R/z) - U_{\text{CPD}}, \quad (5)$$

$$U_{\text{FM}}^{\text{Kelvin}} = \frac{q\delta}{\pi\varepsilon R^2}\frac{(1 + z/R)^2}{(1 + 2z/R)z/R} - U_{\text{CPD}}. \quad (6)$$

In this work, the results are presented assuming the KPFM is operated in the FM mode.

Note that within the approximations made, the direct coupling between local charges, u_0 in equation (2), does not affect the Kelvin voltage since it is independent on the bias U_{dc}. Also, the purely capacitive term u_2 only depends on the tip-surface geometry. Therefore, any effects that fixed charges in the system have on the Kelvin voltage come through the charge-capacitor coupling, u_1. For instance, in the case of point charge q' on the surface at distance δ' directly below the tip ($x = 0$) this term would simply be $u_1 = -q'\delta'/z$, symmetrical to the case of a charged tip. Here the minus sign is due to the charge being at a fixed distance from the electrode at potential U (the surface), instead of the electrode at ground (the tip). Therefore, for a charge on the surface directly below the tip, the Kelvin voltage is given by equations (5) or (6), modified by the substitution $q\delta \to -q'\delta'$.

For a charge not on the symmetry axis of the system, estimating the capacitive potential is more difficult and must be done numerically. Also note that according to equations (1) and (2), u_1 is a sum over all charges. Since the Kelvin voltage is proportional to the derivative of u_1, it too must be additive with respect to having multiple charges in the system.

For large tip-surface distances it is justified to ignore geometric relaxations of atoms on the tip and the surface due to chemical tip-surface interactions, even though such effects are expected to be important in obtaining atomic resolution in KPFM measurements [41, 42]. However, we emphasize that our model also ignores changes in the local structure and polarization of the tip and surface due to changes of the total voltage U, which may also be important. For instance, in KPFM on bulk insulators, polarization of the dielectric due to the applied bias plays a crucial part, and so the model is not directly applicable to such systems as yet. To correctly incorporate such effects, the macroscopic polarization and electric field of the capacitor should be calculated and imposed on the atomic model [43]. Also note that in a case where the approximation of the static geometry fails, the coefficients u_i in equation (2) are no longer U independent and the strict parabolic relationship between energy and bias may break down.

III. RESULTS

A. Force spectroscopy

In Figure 2, calculated force spectroscopy curves are presented for oxygen (red), magnesium (blue), and silver (gray) tips on Ag and MgO/Ag surfaces. For the Ag surface, the forces obtained above the Ag site (a) and hollow site (b) are shown. The general behavior is found to be the same for all tips. Especially, the Mg and Ag terminated tips experience quite similar forces, while the O tip feels stronger attraction. On the hollow site, one needs to approach closer to the surface to reach the region of strong attraction, simply because the distance between surface Ag atoms is quite large, and the tip apices fit inside the empty region between the Ag atoms.

On the Ag-supported MgO monolayer, forces above the Mg (c) and O sites (d) are shown. On the Mg site, strong attraction is found for the O tip. This is expected, since the O tip is terminated with a negatively charged ion and the Mg ion on the surface has a positive charge. A positively terminated Mg tip, on the other hand, feels only a weak attraction until very close to the surface when the tip jumps to contact. Also the Ag tip experiences very weak forces. On the O site, the situation is reversed: the O tip measures only weak forces while there is a deep minimum in the force curve obtained for the Mg tip. Again, the forces calculated for an Ag tip resemble those obtained for an Mg tip, although the absolute strength of the force in the attractive region is weaker.

Above, the MgO tips were constructed to be stoichiometric so as to make them charge neutral. However, it is also interesting to consider non-stoichiometric MgO tips. No electrons are added or removed from the calculations to maintain charge neutrality of the entire system, but having excess Mg or O ions in the tip does induce strong dipole moments on the tips pointing either towards the surface or away from it. Furthermore, there is charge transfer between the top of the MgO monolayer and the

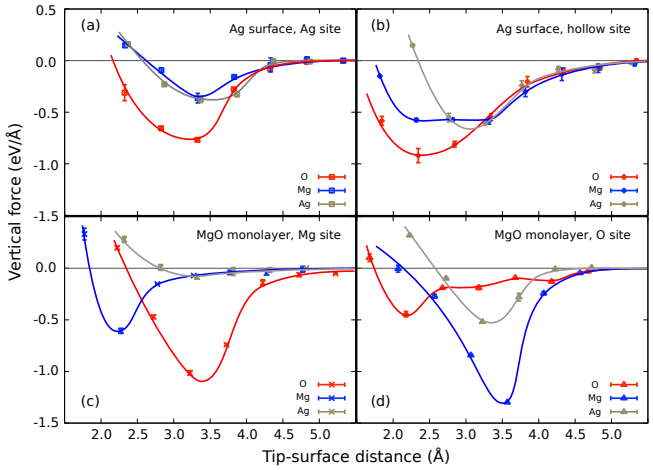

FIG. 2: Calculated force spectroscopy curves for O (red), Mg (blue), and Ag-terminated (gray) tips on the Ag (a) and hollow sites (b) on an Ag surface and the Mg (c) and O sites (d) on an Ag-supported MgO thin film. The lines are only visual aids. Note that the forces represent only the short-range part of the overall tip-surface interaction (no contribution of the macroscopic tip and surface).

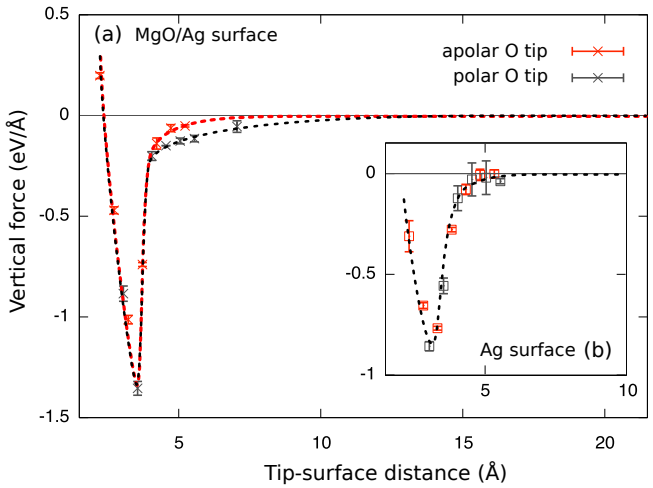

FIG. 3: Calculated force spectroscopy curves for polar (black, $Mg_{32}O_{32}$ cluster, dipole: 1 Debye) and non-polar (red, $Mg_{29}O_{31}$ cluster, dipole: 8 Debye) oxygen-terminated tips on MgO/Ag (a) and Ag (b) surfaces. The lines are only visual aids. Note that the forces represent only the short-range part of the overall tip-surface interaction (no contribution of the macroscopic tip and surface).

Ag substrate, so that the thin film becomes a dipole layer which may interact with a polar tip even at large separations via electrostatic dipole-dipole coupling [12, 44]. The calculated dipole strength of the film is about 0.03 eÅ/ion (about 0.5 Debye per surface unit cell), making the effective dipole moment of the layer several Debye as an entire area beneath the tip contributes to the interaction. Note though, that the electric field of a uniformly charged plane is homogeneous and will not exert a force on a dipole. Here, however, we are examining a region where the inter-ionic separations are comparable to the distance of the tip from the surface and the complicated inhomogeneous electric potential is determined in the calculations.

Extrapolated long range force curves obtained with a stoichiometric and a non-stoichiometric oxygen terminated tip are compared in Figure 3 for the MgO/Ag [Mg site, (a)] and Ag [Ag site, (b)] surfaces. For the plain silver surface, both tips exhibit similar forces and neither feels a force beyond the limit of chemical interactions, roughly 5 Å above the surface. On the MgO monolayer, the short range forces are again quite similar. This is expected as the local structure and chemical properties of the tip apices are almost the same. At long tip-surface distances, however, the force curve of the strongly polar non-stoichiometric tip shows a tail of a weak attractive interaction. For the stoichiometric tip, the force decays much more rapidly.

Our results confirm those of Ref. 12, where it was shown that long range tip-surface interactions, such as those found here, can lead to substantial contrast shifts in topography images. The contrast change occurs simply because the long range coupling appears strongest when both the tip and the surface carry a dipole. Therefore, imaging the metal and monolayer surfaces with a neutral tip yields the correct contrast, but the apparent height of the monolayer is different when imaged with a polar tip, due to the long range coupling.

B. Kelvin probe force microscopy

In our recent paper [30] we discussed the influence of the tip polarization on the mean Kelvin voltage when the tip scans a conducting surface. The mean Kelvin voltage can be used to distinguish positive from negative and polar from neutral tips. In the next Section we enlarge our studies and discuss the case when a thin polar layer is placed between tip and surface as is the case for thin MgO films on the Ag(001) surface. Furthermore, because placing a charge or a dipole on the surface (tip uncharged) is, in principle, symmetric to having a charge or dipole at the tip apex (see Section II B), we use our model to describe also charges on surfaces due to their general relevance in KPFM of insulating materials.

1. *Charges/dipoles at the tip*

In Figure 4 (a), the calculated Kelvin voltages are plotted as a function of tip distance, assuming a zero U_{CPD} for simplicity. We consider a positive tip, which carries either an (additional) Mg^{2+} ad-ion or an MgO dipole. The considerable large shifts in the voltage are due to the charged and polar tips above the metallic surface. The analytic expression (6) for the Mg^{2+} charged tip is also plotted and matches perfectly the numerical results. In the same figure, similar shifts are plotted for the Mg^{2+} tip above an MgO monolayer island: one curve was calculated for the case that the tip is placed above an MgO step and the other curve was obtained for a tip positioned above a flat MgO terrace. Remarkably, for an Mg^{2+} charged tip the Kelvin voltage is almost the same for all three surfaces — metal, MgO monolayer, and step — within numerical accuracy.

However, in the previous analysis the monolayer of MgO is treated as a non-polar layer. Previous theoretical [44] and experimental studies [12, 45] have shown that

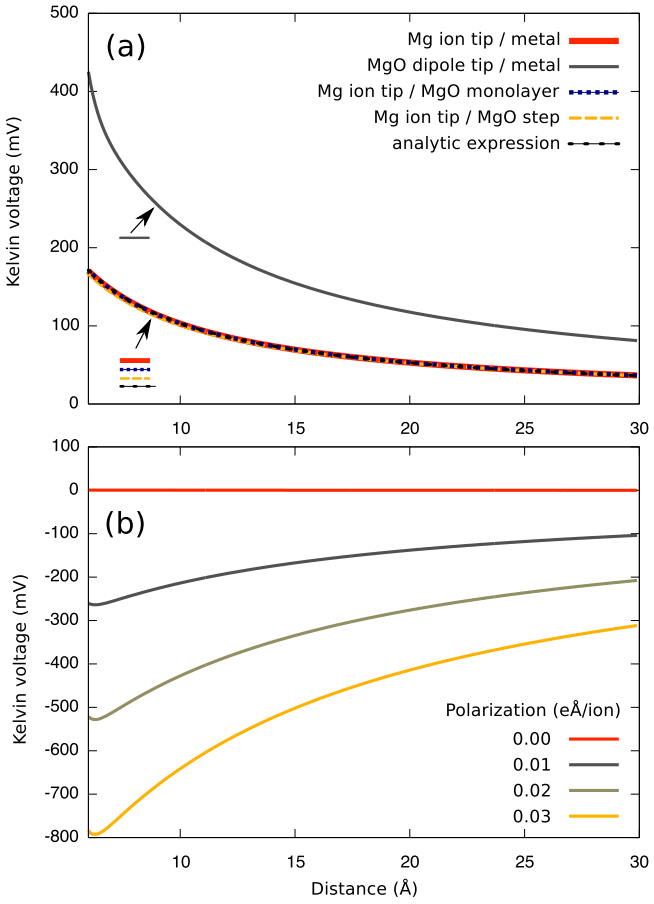

FIG. 4: Calculated shifts in Kelvin voltages ($U_{\mathrm{CPD}} = 0$ V) for a $R = 10$ nm tip, as a function of tip-surface distance. (a) Charged (red) or polar (black) tips on a metal surface and the same charged tip over an MgO monolayer (gray) and a step (yellow). The shift obtained from equation (6) for the Mg^{2+} ion tip is also shown (brown). All the curves calculated with the Mg^{2+} ion tip, including the analytic expression, are almost the same and difficult to distinguish in the figure. (b) A metal tip on an MgO monolayer, where the layer changes from non-polar (red) to increasingly polar (black, gray, yellow).

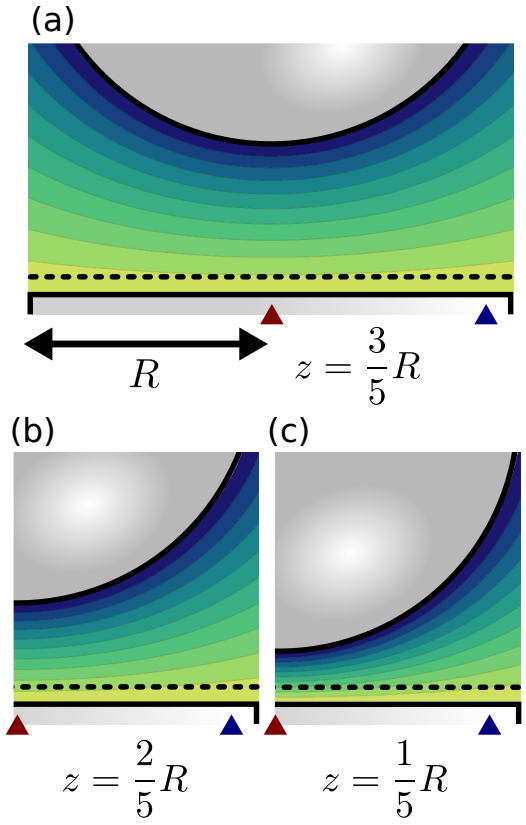

FIG. 5: Characteristic equipotential maps for three different tip-surface distances (a) $3R/5$, (b) $2R/5$, and (c) $R/5$. The dotted line is at the same height in all figures. Under the tip (red triangle), the potential at the marked height changes rapidly as the tip approaches. Aside from the tip (blue triangle), potential at the marked height is only weakly dependent on tip height.

charge transfer between the monolayer and metal results in a dipole at the surface. In Figure 4 (b), the Kelvin shift calculated with a metallic (non-charged) tip is shown for different MgO monolayers at terrace sites, each of which have different dipoles. The polarization is controlled simply by shifting the O^{2-} ions towards the surface, creating a dipole moment pointing away form the surface, which in turn effectively reduces the work function of the silver surface. Note that the curve for 0.03 eÅ/ion represents the expected value for a real monolayer of MgO on the Ag(001) surface based on our first principles calculations of the dipole.

For the non-polar MgO layer (red curve), the Kelvin voltage is not affected, and because the tip is neutral, it does not contribute to the voltage either. When the layer has a static dipole, the Kelvin voltage is shifted towards negative values whereas the shift depends linearly on the strength of the polarization. All this perfectly agrees qualitatively with KPFM experiments, which show indeed a reduction of the Kelvin voltage at one monolayer thin MgO islands compared to the Ag surface [12]. Since the Kelvin voltage is additive, measuring the voltage with a charged tip on a polar surface yields directly the sum of the contributions from the tip charge and surface polarization. Therefore, a charged tip will in general not measure the true work function, however, such a tip should still produce similar changes in the Kelvin voltage due to surface polarization as a metallic tip.

2. *Local charges/dipoles on the surface*

Even if a charge on the surface is imaged with a neutral tip, the charge still couples to the capacitor formed by the tip and the surface. This effect caused by the long-range electrostatic tip-surface interaction is an important aspect in KPFM in general and will therefore be quantified in this Section.

The formation of Kelvin contrast can be qualitatively understood by examining Figure 5, where isosurfaces of the capacitive potential ($\phi(U)$ from equation (1)) are plotted for different tip distances (no point charges in the system). Now, consider introducing a point charge in the capacitive potential. According to equations (3) and (4), the measured shift in Kelvin voltage is proportional to the first or second derivative of the potential felt by the charge, u_1 in equation (2), with respect to the tip distance z. In the figure, we see that directly under the tip (marked with a red triangle), the potential changes linearly when

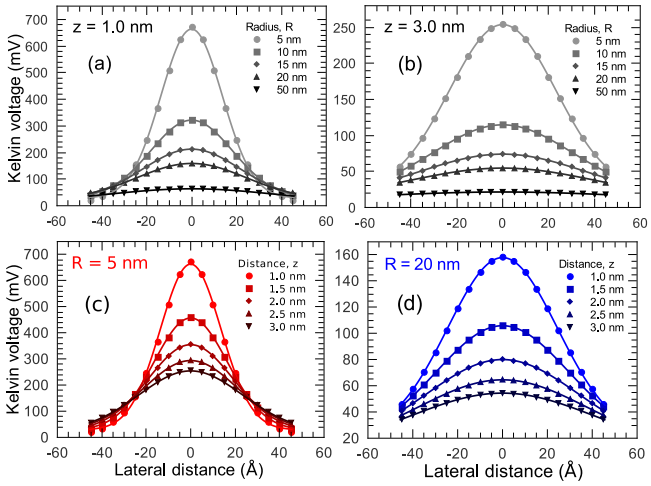

FIG. 6: Calculated Kelvin voltages ($U_{\mathrm{CPD}} = 0$ V) as a function of lateral distance on the surface (lateral Kelvin profiles). The voltages were calculated for a metallic tip above a metal surface on which a single negative charge (-2 e) is placed at a distance of 2 Å from the surface. (a,b) Tips of various radii at a distance of 1.0 nm (a) and 3.0 nm (b) above the surface. (c,d) Distance dependent Kelvin profiles for a $R = 5$ nm sharp (a) and $R = 50$ nm blunt tip (b). The curves are Gaussian fits to the data.

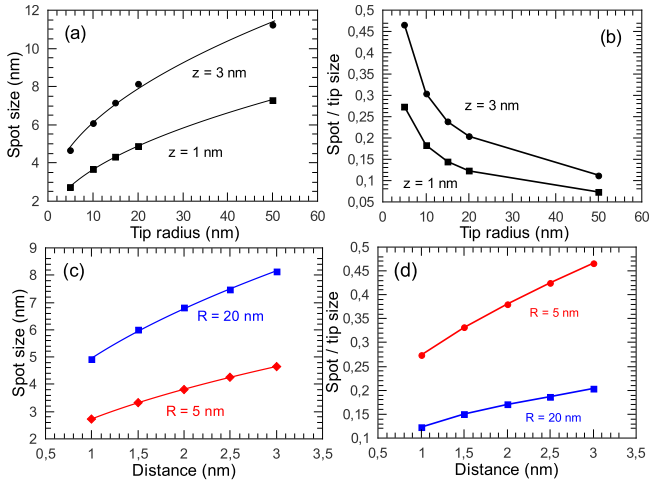

FIG. 7: (a,b) The spot size and the ratio spot-to-tip size as a function of the tip radius. (c,d) The distance dependency of the spot size and the ratio spot-to-tip size. The spot size is the width at half-maximum taken from the curves shown in Fig. 6.

moving between surface and tip. At a fixed distance from surface (line in the figure), the potential depends strongly on the tip-surface distance. Thus, having a point charge directly below the tip will result in a large Kelvin voltage. However, if the charge is located not directly below the apex, but to the side of it (blue triangle), it remains nearly at the potential of the surface even when the tip approaches, simply because the surface of the spherical apex remains distant. Then, u_1 is nearly constant in z, and the Kelvin voltage is small.

The four graphs in Figure 6 show lateral profiles of the Kelvin voltage, which is plotted as a function of the lateral distance x between the tip and the point charge (see Figure 1) for various tip radii and distances. The charge is an O^{2-} ion, which is located by $\delta' = 2$ Å from the surface. A comparison of (a) and (b) shows that the Kelvin voltage is larger for shorter distances (a) than for larger ones (b). For the sharp tip close to the surface ($R = 5$ nm, $z = 1$ nm), the Kelvin voltage clearly peaks when the tip is directly above the surface charge ($x = 0$). But even then the peak width is of the order of some nanometers, which is comparable to the size of the tip. For symmetric tips, as modeled here as a spherical tip, the Kelvin profile of the charge translates into a nanometer sized spot with a symmetric shape, the intensity of which decreases monotonously in all directions.

For a blunt tip ($R = 20$ nm), the lateral resolution of the Kelvin voltage is very low - the spot size is larger by a few nanometers in comparison to the sharp tip. This is because the electric field of the capacitor is nearly uniform and perpendicular to the surface when a blunt tip is close to the conductive surface. Therefore, the capacitive potential ($\phi(U)$ in equation (1)) is nearly constant when moving parallel to the surface, while it depends strongly on the distance from the surface. Note that in the extreme case, when the radius is very large, the tip-surface system can be considered as a plate capacitor and $\phi(U)$ is constant with respect to x.

The dependence of the spot size on the tip size is in particular visible when the tip is close to the surface (a) in comparison when the tip is farther away (b). The distance dependence of the spot size is shown specifically in Figure 6 (c) and (d) for the sharp ($R = 5$ nm) and blunt tip ($R = 20$ nm), respectively. The spot size widens considerably when the tip-surface distance grows and becomes comparable to the tip size (c). For blunt tips, the spot size is quite large even for small tip-surface distances (d), although the maximum Kelvin voltage changes drastically as in the case of the sharp tip.

For quantifying the spot size, the data in Figure 6 were fitted to Gaussian functions (curves). As can be seen, the curves almost perfectly describe the contours of the Kelvin profiles (Fig. 6). We define the spot size as the lateral width at half maximum of the Gaussian curve.

The spot size and the ratio of spot width to tip diameter (spot-to-tip size) are plotted as a function of the tip radius in Figure 7 for a constant distance of 1.0 and 3.0 nm. Note that the ratio does not yield a direct statement about the lateral resolution — it merely shows how the "effective" size of the tip relates to the real physical size. The spot size is an absolute measure of lateral resolution. Still, it is interesting to plot the spot-to-tip ratio as one may expect the lateral resolution of the KPFM to depend on tip size [46].

As expected, the spot size increases with increasing tip radius (a). The spot size is roughly proportional to $\sqrt{R}$, which is similar to the result of Ref. 47 for force resolution. Further, the more the radius of the tip increases, the smaller is the effective part of the tip apex which actually contributes to the Kelvin voltage, as the spot-to-tip size ratio scales according to $1/\sqrt{R}$ (b). If the distance dependence of the same quantities is analyzed for the sharp ($R = 5$ nm) and blunt tip ($R = 20$ nm), it can be further seen that the spot size increases with increasing distance, again approximately $\sim \sqrt{z}$ (Fig. 7 (c) and (d)). At the limit of having the tip far from the surface, the spot size should in principle diverge as the Gaussian peak in the

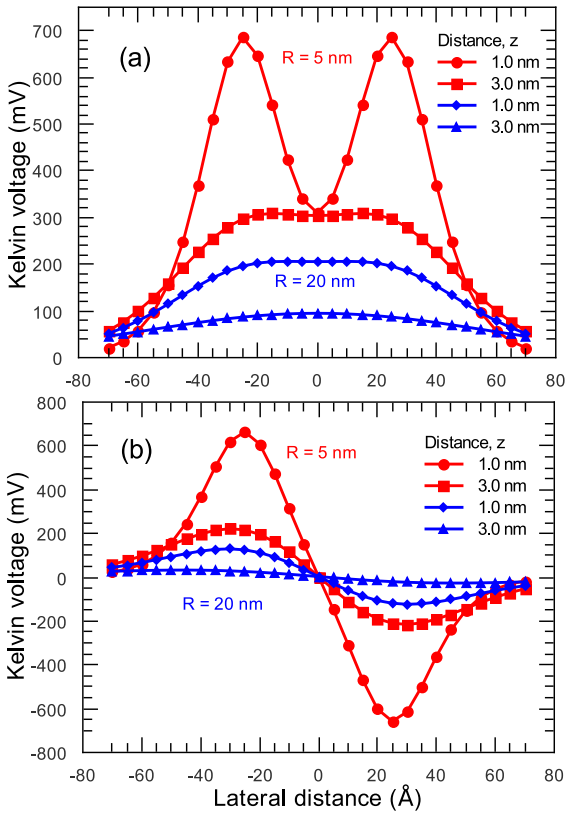

FIG. 8: Lateral resolution in KPFM when fixed surface charges are imaged, which is exemplified by two surface charges at a distance of 5 nm on the surface. Shown are profiles of the Kelvin voltage for a sharp (red curves) and blunt tip (blue curves) at two distances ($z = 1$ and 3 nm). (a) Both charges are O^{2-} ions (same sign) (b) The left charge is an O^{2-} ion, the right one an Mg^{2+} ion.

Kelvin voltage becomes ever lower and wider.

As a rule of thumb it can be said that the lateral size of a point charge in a KPFM image is of the order of the tip radius when the tip is at a distance of roughly the tip radius from the surface. The size of the spot decreases when the tip approaches the surface.

The latter results have large consequences on the resolution when surface charges are imaged with the Kelvin microscope. Figure 7 (c) shows that at a distance of 1 nm the resolution of the blunt and sharp tip is around 5 and 3 nm, respectively, if the spot size is taken as a measure for the resolution. In order to verify this, we also model the case where two charges are on the surface. Figure 8 shows the lateral Kelvin profiles for a tip that scans over either (a) two charges with same strength and sign (two O^{2-} ions) or (b) two charges with same strength, but opposite sign (an O^{2-} and Mg^{2+} ion). The two charges are at a lateral distance of 5 nm on the surface, with a distance of $\delta' = 2$ Å from the surface in vertical direction.

At a tip-surface distance of 3 nm, the blunt tip does not resolve the equivalent charges, but images them rather as a fuzzy and long feature (Fig. 8 (a)). Even if the blunt tip is approached to a distance of 1 nm, the two charges are imaged as a plateau. The same low resolution can be observed for the sharp tip, when placed at a distance of 3 nm. However, as soon as the tip is brought to a distance of 1 nm, the two charges are clearly resolved by the sharp tip. Note that the distance of both charges is not correctly represented — they are imaged with a distance that is slightly smaller than the true distance. The reason is that the tip feels maximum interaction when it is almost above one of the charges, but such that it already feels the other charge. This effect certainly diminishes when the distance between the charges is increased - the correct distances are then measured.

When the opposite charges are imaged (Fig. 8 (b)), we have a different situation. The sharp tip resolves the two charges at any distance. Since the charges have opposite signs, the positive charge changes the sign of the Kelvin voltage to negative. The blunt tip does not yield a large Kelvin voltage at large distances (3 nm). This is because the contributions from the two charges almost cancel each other. However, when the blunt tip gets closer to the surface (e.g. at 1 nm), it indeed resolves and even distinguishes both charges.

The profiles in Figure 8 show that the width of the spot can be used as a rough measure for the resolution in the KPFM imaging of charges. The lateral resolution in the imaging of surface charges in KPFM is best when the tip apex is small and close to the surface. In the special case, when the charges have opposite signs, the resolution is slightly better.

IV. SUMMARY

In this work, we present numerical simulations of the chemical short-range and electrostatic long-range interaction between different types of tips with a silver surface and supported MgO monolayers. Our simulations show that atomic resolution can be obtained with silver and MgO tips on both, the silver surface and MgO monolayers, at tip-surface distances of less than 5 Å. At larger distances, the chemical interaction between the tip apex and the surface disappears and no atomic resolution can be obtained.

As soon as neutral, charged or polar tips couple to charges or dipoles on the surface, a long-range electrostatic interaction is produced. The polarization can be directly detected by using KPFM, which is exemplified by thin MgO monolayers of different net polarizations. If the MgO monolayer has no net dipole, no difference in the Kelvin voltage can be observed between the silver and MgO/silver surface, independent on if the tip is charged, polar or neutral. This is due to the contributions from opposite charges (cations and anions in the film) canceling. However, as soon as the MgO layer has a net dipole, a Kelvin shift can be observed in agreement with experimental observations.

Local charges or dipoles in the tip are also detected by KPFM, similarly to ones on the surface. However, contrary to nc-AFM (force spectroscopy) which detects the coupling between charges in the tip and on the surface, KPFM directly detects charges or dipoles in the tip or on the surface as shifts in the Kelvin voltage. In particular, the contributions from tip and surface charges are detected separately in KPFM (nc-AFM detects the complicated interaction between the two), and if charges are present both in the tip and on the surface, their contributions to the Kelvin voltage are simply linearly added

together.

It is shown that fixed point charges on the surface are imaged as large spots in Kelvin images. The size of a spot increases with the size of the tip and the tip-surface distance. The lateral resolution of surface charges in KPFM is discussed by considering two surface charges. A slightly better resolution is obtained when the charges have opposite signs in comparison to the same signs. For a good resolution, very sharp tips are needed, which must be brought close to the surface.

The results presented in this work deal with dipoles and charges on a conducting silver surface. This is important in general for detecting charged defects in thin films on metal surfaces like F centers in MgO(001) by KPFM. Charged defects also appear especially on bulk insulator surfaces and could have been already detected by KPFM. The results are also directly relevant to imaging of charged atoms or molecules on thin insulating films [32, 48]. We believe that our model forms a good starting point for the modelling of bulk insulator surfaces in future, including the full effect of bias induced atomic displacements.

Acknowledgments

Stimulating discussion with P. Girard, Th. Mélin, A. L. Shluger, L. Kantorovich, A. Baratoff, C. Henry, F. Esch and U. Heiz are highly acknowledged. We also acknowledge financial support through the FANAS project NOMCIS. TJH and ASF acknowledge support from the Academy of Finland via its Centre of Excellence programme, as well as the computational resources offered by CSC, Finland.

[1] M. Nonnenmacher, M. P. O Boyle, and H. K. Wickramasinghe, Appl. Phys. Lett. **58**, 2921 (1991).
[2] J. M. R. Weaver and D. W. Abraham, J. Vac. Sci. Technol. B **9**, 1559 (1991).
[3] P. Girard, Nanotechnology **12**, 485 (2001).
[4] V. Palermo, M. Palma, and P. Samori, Adv. Mater. **18**, 145 (2006).
[5] R. Berger, H. J. Butt, M. B. Retschke, and S. A. L. Weber, Macromol. Rapid Commun. **30**, 145 (2009).
[6] *Noncontact Atomic Force Microscopy*, Eds. S. Morita, R. Wiesendanger, and E. Meyer (Springer-Verlag, Berlin, 2002).
[7] A. Kikukawa, S. Hosaka, and R. Imura, Rev. Sci. Instrum. **67**, 1463 (1996).
[8] S. Kitamura and M. Iwatsuki, Appl. Phys. Lett. **72**, 3154 (1998).
[9] C. Sommerhalter, T. W. Matthes, T. Glatzel, A. Jäger-Waldau, and M. C. Lux-Steiner, Appl. Phys. Lett. **75**, 286 (1999).
[10] F. Krok, J. J. Kolodziej, B. Such, P. Czuba, P. Struski, P. Piatkowski, and M. Szymonski, Surf. Sci. **566**, 63 (2004).
[11] C. Loppacher, U. Zerweck, and L. M. Eng, Nanotechnology **15**, 9 (2004).
[12] M. Bieletzki, T. Hynninen, T. M. Soini, M. Pivetta, A. S. Foster, F. Esch, C. Barth, and U. Heiz, Phys. Chem. Chem. Phys. **12**, 3203 (2010).
[13] M. Goryl, F. Krok, J. J. Kolodziej, P. Piatkowski, B. Such, and M. Szymonski, Vacuum **74**, 223 (2004).
[14] U. Zerweck, C. Loppacher, T. Otto, S. Grafström, and L. M. Eng, Nanotechnology **18**, 84006 (2007).
[15] H. O. Jacobs, P. Leuchtmann, O. J. Homan, and A. Stemmerb, J. Appl. Phys. **84**, 1168 (1998).
[16] T. Glatzel, L. Zimmerli, S. Koch, B. Such, S. Kawai, and E. Meyer, Nanotechnology **20**, 264016 (2009).
[17] G. H. Enevoldsen, T. Glatzel, M. C. Christensen, J. V. Lauritsen, and F. Besenbacher, Phys. Rev. Lett. **100**, 236104 (2008).
[18] C. Barth and C. R. Henry, Nanotechnology **17**, S155 (2006).
[19] C. Barth and C. R. Henry, Phys. Rev. Lett. **98**, 136804 (2007).
[20] C. Barth and C. R. Henry, Appl. Phys. Lett. **89**, 252119 (2006).
[21] C. Barth and C. R. Henry, J. Phys. Chem. C **113**, 247 (2009).
[22] B. D. Terris, J. E. Stern, D. Rugar and H. J. Mamin, Phys. Rev. Lett. **63**, 2669 (1989).
[23] E. B. Bussmann, N. Zheng and C. C. Williams, Nano Lett. **6**, 2577 (2006).
[24] S. S. P. Parkin, C. Kaiser, A. Panchula, P. M. Rice, B. Hughes, M. Samant, and S.-H. Yang, Nature Mater. **3**, 862 (2004).
[25] S. Yuasa, T. Nagahama, A. Fukushima, Y. Suzuki, and K. Ando, Nature Mater. **3**, 868 (2004).
[26] *Nanocatalysis*, Eds. U. Heiz and U. Landman (Springer-Verlag, Berlin, 2006).
[27] H. J. Freund and G. Pacchioni, Chem. Soc. Rev. **37**, 2224 (2008).
[28] C. Harding, V. Habibpour, S. Kunz, A. N. S. Farnbacher, U. Heiz, B. Yoon, and U. Landman, J. Am. Chem. Soc. **131**, 538 (2009).
[29] M. E. Vaida, T. M. Bernhardt, C. Barth, F. Esch, U. Heiz, and U. Landman, Phys. Status Solidi B **247**, 1001 (2010).
[30] C. Barth, T. Hynninen, M. Bieletzki, C. R. Henry, A. S. Foster, F. Esch, and U. Heiz, New J. Phys. **12**, 093024 (2010).
[31] L. Giordano, U. Martinez, G. Pacchioni, M. Watkins, and A. L. Shluger, J. Phys. Chem. C **112**, 3857 (2008).
[32] F. Bocquet, L. Nony, and C. Loppacher, preprint (submitted to Phys. Rev. B).
[33] G. Kresse and J. Furthmuller, Phys. Rev. B **54**, 11169 (1996).
[34] H. J. Monkhorst and J. Pack, Phys. Rev. B **54**, 11169 (1976).
[35] L. N. Kantorovich, A. I. Livshits, and M. Stoneham, J. Phys. Condens. Matter **12**, 795 (2000).
[36] L. N. Kantorovich, A. S. Foster, A. L. Shluger, and A. M. Stoneham, Surf. Sci. **445**, 283 (2000).
[37] Th. Glazel, S. Sadewasser, and M. C. Lux-Steiner, Appl. Surf. Sci. **210**, 84 (2003).
[38] U. Zerweck, C. Loppacher, T. Otto, S. Grafstrom, and L. M. Eng, Phys. Rev. B **71**, 125424 (2005).
[39] T. Takahashi and S. Ono, Ultramicroscopy **100**, 287 (2004).
[40] S. Hudlet, M. Saint Jean, C. Guthmann, and J. Berger, Eur. Phys. J. B **2**, 5 (1998).
[41] L. Nony, A. S. Foster, F. Bocquet, and Ch. Loppacher, Phys. Rev. Lett. **103**, 036802 (2009).
[42] S. Sadewasser, P. Jelinek, Ch. Fang, O. Custance, Y. Yamada, Y. Sugimoto, M. Abe, and S. Morita, Phys. Rev. Lett. **103**, 266103 (2009).
[43] S. Sadewasser, C. Leendertz, F. Streicher, and M. Ch.

Lux-Steiner, Nanotechnology **20**, 505503 (2009).
[44] L. Giordano, F. Cinquini and G. Pacchioni, Phys. Rev. B **73**, 045414 (2006).
[45] T. König, G. H. Simon, H.-P. Rust, and M. Heyde, J. Phys. Chem. C **113**, 11301 (2009).
[46] S. Ono and T. Takahashi, Jpn. J. Appl. Phys. **43**, 4639 (2004).
[47] S. Belaidi, P. Girard, and G. Leveque, J. Appl. Phys. **81**, 1023 (1997).
[48] L. Gross, F. Mohn, P. Liljeroth, J. Repp, F. J. Giessibl, and G. Meyer, Science **324**, 1428 (2009).